Journal of the Korean Nuclear Society
Volume 9, Number 4, December, 1977

<Original>

Mechanical and Thermal Analysis of Oxide Fuel Rods

Ilsoon Hwang*, Byungho Lee** and Changkun Lee*

(Received December 3, 1977)

Abstract

An integral computer code has been developed for a mechanical and thermal design and performance analysis of an oxide fuel rod in a pressurized water reactor. The code designated as FROD 1.0 takes into account the phenomena of radial power depression within the pellet, cracking, densification and swelling of the pellet, fission gas release, clad creep, pellet-clad contact, heat transfer to coolant and buildup of corrosion layers on the clad surface. The FROD 1.0 code yields two-dimensional temperature distributions, dimensional changes, stresses, and internal pressure of a fuel rod as a function of irradiation time within a reasonable computation time. The code may also be used for the analyses of oxide fuel rods in other thermal reactors. As an application of FROD 1.0 the behavior of fuel rod loaded in the first core of Go-ri Nuclear Power Plant Unit 1 is predicted for the two power histories corresponding to steady state operation and Codition II of the ANS Classification. The results are compared with the design criteria described in the Final Safety Analysis Report and a discrepancy between these two values is discussed herein.

요 약

가압수형 원자로에 사용되는 이산화우라 핵연료봉의 역학적 열적설계 및 성능 분석을 위한 종합적 전산 코드가 개발되었다. FROD 1.0으로 명명된 이 코드에는 연료소자에서 반경 방향으로의 출력 침체, 연료소자의 균열, 고밀화 및 팽창, 핵분열기체의 방출, 피복관의 크립, 냉각수에 의한 열전달 및 부식층의 형성 등의 제반 현상이 고려되었다. 이 FROD 1.0 코드로써 이차원적 온도 분포, 변형도, 응력 및 피복관 내압 등이 연소시간의 함수로서 적절한 전산 시간이내에 산출된다. 이 코드는 또한 종류가 다른 열중성자로에 쓰이는 산화 연료에도 응용될 수 있다. FROD 1.0의 응용으로서 원자로의 정상가동 상태와 미국 원자력학회 분류의 제 2 상태에 해당하는 두 가지의 출력 경로에 대하여, 고리 원자력 발전소 1호기의 초기 노심에 장전된 핵연료봉의 연소특성을 예측하였다. 예측결과는 최종 안전 심사 보고서에 기술된 핵연료봉 설계기준과 비교되었으며 둘 사이의 차이점이 논의되었다.

* Korea Atomic Energy Research Institute
** Korea Advanced Institute of Science.

1. Introuduction

The core power capability of pressurized water reactor is usually limited by departure from nucleate boiling, fuel melting, loss of coolat accident and pellet-clad interaction (PCI), etc., Therefore an accurate description of the mechanical and thermal behaviors of fuel rods is essential to sound design and proper management of the reactor core.

A fuel rod for the PWR contains cylindrical fuel pellets vertically stacked in a thin wall-clad tube as sketched in Fig. 1. The sintered uranium dioxide pellets, which are fabricated with dished end faces, have a density about 95% of theoretical value. A soft helical spring in the upper plenum prevents any bulk movement of the pellet stack prior to operation. The fuel rod is pre-pressurized usually with helium gas in order to reduce the pressure difference between inner and outer boundaries of clad and to improve gap conductance.

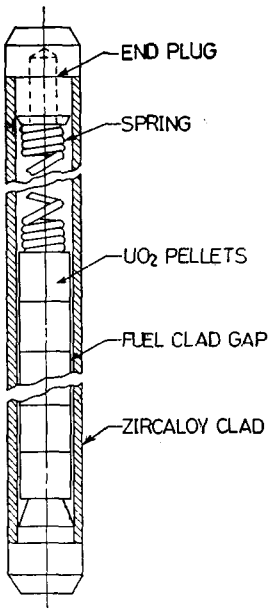

Fig. 1. Fuel Rod Schematic for a Typical Pressurized Water Reactor.

As the reactor starts up, the fuel rods suffer various kinds of damages from the physical and chemical phenomena. A considerable amount of experience with oxide fuel has confirmed that there are two dominant modes of dimensional instability due to irradiation, called densification and swelling. Densification effects have been observed as results of either the disappearance of small pores from the oxide matrix or the migration of fabricated pores toward the center of fuel under the influence of thermal gradient. But the latter encountered at very high temperature is limited to the hotter central regions of pellets and apparent dimensional changes are masked by other physical changes in the pellet at such high temperature. As burnup increases fuel swells due to retention of solid and gaseous fission products. Since the most of stable fission gases are inert gases having poor solubility in the grains, the fission gases are readily to nucleate. They are also subsequently destroyed by fission product spikings[1]. The nucleated gas bubbles are able to move and coalesce under the influence of thermal gradient, eventually some of the fission gases are released to the void space of fuel rod and raise the rod internal pressure. On the other hand the clad deforms due to creep with the presence of high pressure, temperature and fast neutron flux. On the clad surface, corrosion and crud deposits are encountered.

The resultant fuel restructuring and clad damages induce the conspicuous changes in the thermal and mechanical properties of the materials.

Hence it is nearly impossible to treat these intricate and sophisticated behaviors

of fuel rod on a first principle. And it can be committed only to numerical approaches that involve careful handling of a comprehensive amount of mathematical models made up from experimental results and theoretical analyses. Now the present method of analysis is organized into three steps, viz., temperature profile, dimensional instability and fission gas behavior, and mechanical analysis of fuel rods.

2. Method of Analysis

2.1. Calculation of Temperature Profile

The temperature profile may be obtained from the heat conservation equation:

$$\nabla(k\nabla T)+q'''=\rho\ c_p\frac{\partial T}{\partial t} \qquad (1)$$

The following three assumptions are made to solve the above equation;

1) Quasi-steady state temperature distribution—a rapid transient power history can also be investigated in part using the quasi-steady state thermal model if the power history is divided into monotonously increasing and decreasing sections.

2) Axi-symmetric heat flow.

3) No axial heat conduction—error introduced by this assumption is known to be less than 0.5% for most power reactors[2].

Within the pellet we obtain,

$$\int_{T(a)}^{T(r)}k(T)=q'''_a\int_r^a\frac{1}{r}\left[\int_0^r f(r')\cdot r'\cdot dr'\right]dr \qquad (2)$$

where the normalized power distribution funcition $f(r)$ takes into account the radial power depression due to attenuation of thermal neutron flux toward the center of fuel. The normalized power distribution function, which depends on the atomic number density of fissile materials and hence on burnup, is determined by making use of a theoretical calculation of radial distribution of thermal and fast neutron fluxes in the pellet[3]. The integrated thermal conductivity of UO_2 in Eq (2) is adjusted with temperature, porosity and fuel restructuring.

About 97.4% of the total fission energy is converted into heat within the fuel. The heat is transferred from the fuel across the gap to clad via radiation, free convection of gap gas and conduction through the gap gas and the contact spots between fuel and clad. However the effect of free convection is slight enough to neglect. For open gap, the thermal conduction through gas mixture composed of the pre-pressurized and the released gases is estimated by averaging the thermal conductivity effectively weighted by respective mole fraction of gap constitutents[4]. Fuel-clad contact enhances the gap conductance appreciably. Several model[s]5,6 are available to evaluate the contact conductance with the presence of contact pressure between pellet and clad. The resultant models on gap or contact conductance utilize empirical constants which were calibrated with the help of experimental results.

Even though a small amount of heat is generated in the clad mostly due to the irradiation of gamma-rays and fast neutrons, this heat is considered negligible.

On the surface of clad, a layer of oxide is introduced due to dynamic corrosion of clad material by attack of active coolant, and another layer of corrosion product deposits (crud) is built which originates from the inner surface of primary cooling loops and impurities in the coolant. Even though the total thickness of the layers is only a magnitude of mil and temperature drop across them will not be ignored because of their poor thermal conductivities[7]. The

rate of oxide weight gain is related with the corrosion governing temperature, surface heat flux, water chemistry and fast neutron flux.

The amount of crud deposit is somewhat different among the reactors with different system configuration.

To calculate the forced convection heat transfer confficient for Newton's Cooling Law, a Dittus-Boelter correlation[8] is used with the properties of coolant evaluated at bulk fluid condition. The correlation for in-pipe flow has been shown to be conservative for rod bundle geometry[9] adopting the unit cell model characterized by the hydraulic diameter. The onset of nucleate boiling is calculated when the clad surface temperature reaches a few degree above the saturation temperature. The several heat treansfer coefficients are utilized for nucleate boiling region. The axial profile of bulk fluid temperature is determined from energy balance:

$$T_f(z) = T_f(0) + \int_0^z \frac{2\pi c}{mc_p} q''(z')dz' \qquad (3)$$

2.2. Dimensional Instability and Fission Gas Behaior

Early in life, fuel pellets are densified due to disappearance of small porse distributed uniformaly in the as-fabricated fuels. This dimensional change is apparent in direction of fuel axis however with negligible radial shrinkage. Therefore the magnitude of the decrease in fuel stack length is related to the volume decrease due to fuel densification. The rate of densification is a strong function of operating temperature, pellet sintering temperature and fabricated density. Obtainable peak density for fuel in Go-ri unit 1 is expected to be about 96% of the theoretical density. The resultant decrease in fuel stack length burdens the fuel rods with additional linear heat rate.

On the other hand, fuel swells due to the retention of fission products. The dimensional changes due to irradiation growth and irradiation creep are not felt in the isotropic oxide fuels[10]. Fission product swelling contains two separate components associated with solid fission products and gaseous fission products. The swelling due to solid fission products is believed to occur isotropically. Over the wide ranges of typical performance parameters, the amount of solid swelling is in direct proportion to burnup, with a value of 0.35% per 10^{20} fission/cm[11], because the solid fission fragments have little chance to be released from the pellet zone.

About thirty atoms of stable fission gases are produced from every hundred thermal fissions. The rate of gaseous swelling depends on the gas solubilities, nucleated bubble size and the rate of fission gas release. Therefore the temperature is an important factor of gaseous swelling. In here several temperature zones of different grain structure are assorted to account different amount of gaseous swelling. The rate of gaseous swelling is rather low at the beginning of life due to fabricated pores accomodating some of the volvume increase. And the rate increases with further burnup.

The fission gas atoms, uniformly produced over a grain, collect in pores and migrate to the grain boundary toward the temperature gradient. Possible mechanisms for the movement of fission gas bubbles are surface diffusion of matrix atoms around the interface between gas and fuel, together with volume self-diffusion of fuel molecules across the bubbles. The pore migration is

also influenced by strain energy gradients [14]. Small migrating bubbles can be pinned and accumulated on the dislocations and energetic boundaries en route. Some of the pinned bubbles can also be released with the help of intergrannular pellet cracking or as a result of subequent mobilization of coalesced bubbles. A model on these diffusion and pinning phenomena, that showed good agreement with experimental data, is employed to estimate the fraction of fission gas release. Then internal pressure of fuel rod is predicted according to gas state equation for ideal gas mixure in iso-baric equilibrium with the temperture gradient.

2.3. Mechanical Analysis of Fuel Rods.

The pellet dimensional change is calculated taking into account the thermal expansion, densification and swelling, and the clad deformation is computed taking into account the creep and irradiation growth and the elastic deflection due to thermal stress and the pressure differential. The fuel densification and swelling behavior are already described in the preceding section. In the formulation of the equilibrium equations and the compatility equations, three conventional assumptions are made:

1) the pellet and the clad and their associated stresses and strains have an axi-symmetry,

2) the pellet and clad planes perpendicular to their axis remain planes after deformation.

3) the pellet-clad friction and body forces are negligible.

However some amount of errior is inherent due to localized strain concentrations in the vicinity of pellet cracks and ridges and due to the developed ovality of clad during the deformation.

To take pellet cracking into consideration the pellet is idealized to be extremely brittle. Or any strain incompatibilities due to differential exansion of pellet under the high thermal gradient can not be accomodated without cracking.

The pellet cracking improves the gap conductance but reduce the thermal conductivity of pellet[13].

Thermal expansion and swelling of pellet can be transmitted as a dominant source of clad stress after pellet and clad are in contact. The contact pressure $P_{cont.}$ between fuel(Ⅰ) and clad(Ⅱ) was determined by elastic analys is with the help of following interface conditions;

$$\left.\begin{array}{l} 1)\ \sigma_r^{I}(r=a')=\sigma_r^{II}(r=b')=-P_{cont.}, \\ 2)\ a=b \end{array}\right\} \quad (4)$$

The result is

$$P_{cont.}=E_{cont.}(b'-a'),$$

and

$$E_{cont.}=\frac{-E^{I}E^{II}\left(\frac{c'^2}{b'^2}-1\right)}{a'\cdot E^{I}\left[1-\nu^{II}+\frac{c'^2}{b^2}(1+\nu^{II})\right]+b'E^{II}\left(\frac{c'^2}{b'^2}-1\right)(1-\nu^{I})}, \quad (5)$$

where $E_{cont.}$ is called strength coefficient, and a', b' and c' represent the fictious values of a, b and c, respectively, that the fuel rod would have in hot state in absence of contact pressure. But it is evident that the contact pressure does not exsist in the open gap where b' is greater than a'.

Clad stresses are determined taking into account the rod internal pressure, contact pressure, system pressure and thermal load for a long pipe with unrestrained ends as a state of plane stress[14]. Thisis;

$$\sigma_r=\frac{b^2c^2(P_s-P_i-P_{cont.})}{(c^2-b^2)r^2}$$

$$+\frac{(P_i+P_{cont.})b^2-P_sc^2}{c^2-b^2}$$
$$+\frac{E\alpha(T_b-T_c)}{2(1-\nu)\ln\left(\frac{c}{b}\right)}\left[-\ln\left(\frac{c}{r}\right)\right.$$
$$\left.-\frac{b^2}{c^2-b^2}\left(1-\frac{c^2}{r^2}\right)\ln\left(\frac{c}{b}\right)\right] \quad (6)$$
$$\sigma_\theta=-\frac{b^2c^2(P_s-P_i-P_{cont.})}{(c^2-b^2)r^2}$$
$$+\frac{(P_i+P_{cont.})b^2-P_sc^2}{c^2-b^2}$$
$$+\frac{E\alpha(T_b-T_c)}{2(1-\nu)\ln\left(\frac{c}{b}\right)}\left[1-\ln\left(\frac{b}{r}\right)\right.$$
$$\left.-\frac{b^2}{c^2-b^2}\left(1+\frac{c^2}{r^2}\right)\ln\left(\frac{c}{b}\right)\right]$$
$$\sigma_z=\tau_{r\theta}=\tau_{\theta z}=\tau_{rz}=0$$

The creep of Zircaloy clad for the very slow strain rate of importance in nuclear reactors, includes irradiation-enhanced creep and the growth-directed irradiation creep as well as thermal creep. The irradiation-enhanced creep is due to the promotion of the stress relaxation in the presence of fast flux. The irradiation-creep depends only upon the fast neutron fluence and the strain can be estimated by some power of fluence. Then the creep rate is evaluated at the averaged values of temperature and effective stress of Von Mises Criterion[15].

2.4 Numerical approach

Since all the models, constitutive formulations and the material properties are implicated and inter-connected to each other, it is required to approach to the solution by means of numerical method. This is achieved by a FORTRAN Ⅳ program, FROD 1.0 which has been developed to examine the in-core behavior of fuel rods.

For computational purpose the stack of pellets is assumed to have been divided into slices. The slices containing pellets are, in turn, divided into several coaxial rings in the radial direction.

A group of flexible information is left for the input requirements such as geometric parameters, rod internal pre-pressurization, flow rate and inlet temperature of coolant, power history and axial power shape, etc. For each stage of irradiation time, the FROD 1.0 code calculates two dimensional temperature profile and dimensional change in pellet and clad, stress distribution in clad, amount of fission gas released and the rod internal pressure.

The whole iterations are based on the method of secant. For the convergence of a typical problem, about five minutes of computation time is required with CYBER-73 series machine.

3. Application of FROD 1.0 to the Analysis of Fuel Rods in the First Core of Go-ri Unit 1

3.1. Input Preparation

The fundamental input parameters are summarized in Table 1[16].

Based on the postulation that fuel rod at the higher power and burnup will carry usually the heavier mechanical, thermal and metallurgical duties, the in-core performance of the all the fuel rods may be thought sound if the fuel rods at the maximum power and the maximum burnup satisfy all the prescribed design criteria for both the steady state operation and transient power histories corresponding to Condition Ⅰ and Ⅱ of the ANS Classification, respectively.

Now the fuel rods of maximum power during the first cycle are selected for examinations. In order to obtain the maximum power histories for steady state operation, the hot channel factors with a following

Table 1. Fuel Design Parameters of Go-ri unit 1

Design Parameters	Value
Average Linear Heat Rate, kW/ft	6.46*
Heat Flux Hot Channel Factor	2.32
Peak Linear Power Resulting from Transient/Operator Errors, kW/ft	20.3
Pellet Density (% of theoretical)	95.0
Pellet Diameter, in.	0.3659
Clad Outside Diameter, in.	0.422
Clad Thickness, in.	0.0243
Fuel Rod Pitch, in.	0.556
Nominal Inlet Temperature, °F	541.2
Coolant Average Mass Velocity, lb/hr-ft^2	2.40×10^6
Nominal System Pressure, psi.	2250.

*For the fresh fuel which is not densified yet.

inter-relationship are useful;

$$F_Q^T=\max\left\{F_{XY}^N\times F_Z^N\times F_U^N\times F_Q^E\right\} \qquad (7)$$

The rod-wise nuclear radial hot channel factors F_{XY}^N and their histories with burnup were obtained from the nuclear design calculation for the first cycle of Go-ri unit 1. However it is not possible, at the time of this work, to determine the accurate power histories for cycles 2 and 3 since there is no specific information of core configuration after reloadings at the end of cycles 1 and 2. However a possible power history may be used allowing some deviation from the real one but without introducing significant errors in the performance evaluation if its burnup is calibrated to the target burnup. On this basis the guessed power histories are generated for the later two cycles.

And the rod-wise maximum power histories are shown in Fig. 2 for steady state operation up to the end of cycle 3.

The nuclear axial hot channel factor F_Z^N is concerned with axial power shape of the fuel rod. The axial power shape varies continually with fuel burnup, xenon oscillation and insertion of control bank. And the shape is not smooth owing to local power depressions at the grid locations and local power spikes at the pellet-to-pellet gaps enlarged by fuel densification. But to save computer time, a smooth curve of fixed axial power distribution is obtained as a time-average shape. The axial power distribution has a value of 1.2 for the nuclear axial hot channel factor as illustrated in Fig. 3. A parametric study showed that the use of the fixed axial power shape re-

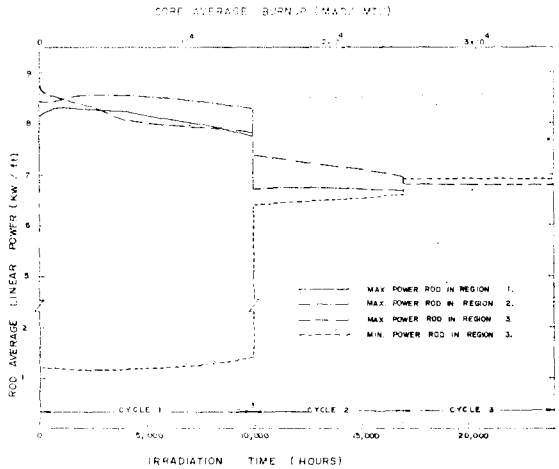

Fig. 2. Rod wise Power Histories of the Steady State Operation of the First Core of Go-ri Unit 1.

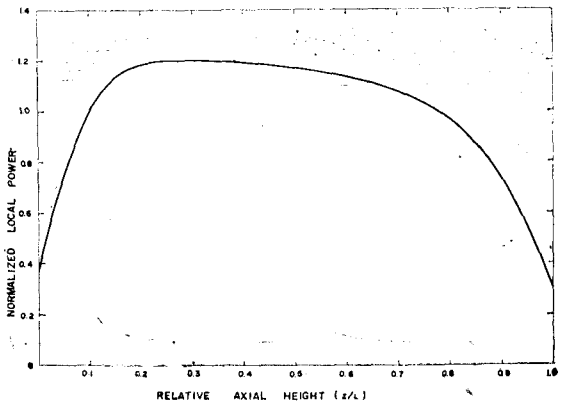

Fig. 3. Fixed Axial Power Shape of Fuel Rods in the First Core of Go-ri Unit 1.

sults in a small difference comparing with the time-varying power shapes.

The uncertainty in hot channel factor F_U^N is introduced to compensate the measurement uncertainty associated with flux mappings by movable in-core detectors. The engineering hot channel fact of F_Q^E is the allowance for heat flux required for local variation in enrichment, pellet density and diameter, surface area of fuel rod and eccentricity of the gap. Thus F_U^N and F_Q^E are not affected by fuel burnup and have the constant design values of 1.05 and 1.03, respectively, for the first core of Gori unit 1.

Overpower transients consistent with ANS Condition Ⅱ events may be caused byco ntrol bank malfunction, erroneous boration/dilution and/or operator errors which must be analyzed to assure that no fuel damage will occur. Under these abnormal environments, an overpower is assumed to start from the steady state operation at the fuel rods which have never experienced any overpower accident in the past.

The maximum local power density corresponding to 118% of reference power is designed to be 20.3 kW/ft as in Table 1. This overpower limit is examined with a tentative power escalation rate of about 0.2 kW/ft-min or 15% of full power per hour.

In the study of overpower events, a fuel rod of the minimum power during the first cycle is additionally examined because sometimes it possesses the higher potential of local power peaking than the maximum power rods under the same condition Ⅱ. The minimum power rod begins its life from the region 3 and is planned to burn through the three cycles. Hence its power histories for later two cycles are guessed again as shown in Fig. 2.

3.2 Fuel Rod Design Criteria

The integrity of the fuel rods under consideration is known to be ensured by designing them so that the following conservative design criteria are satisfied during Condition Ⅰ (including load follow as well as steady state operation) and Condition Ⅱ over the fuel life time[16]:

1) In order to prevent fuel melting, the maximum temperature in the fuel shall not exceed the melting point of fuel. However the minimum margin between the center temperature of the hottest pellet and melting temperature of uranium dioxide occurs at the beginning of life.

$$(T_0)_{BOL.} < 5080°F \tag{8}$$

2) The clad surface temperature T_c shall not exceed the following temperature limits to avoid excessive external corrosion.

$$T_c < \begin{cases} 750°F \text{ under steady-state} \\ 800°F \text{ during transient event.} \end{cases} \tag{9}$$

3) In order to prevent failure due to successive creepout of clad, the internal gas pressure is less than the nominal coolant design pressure, P_s, i.e.

$$P_i < P_s. \tag{10}$$

4) The clad tensile strain is less than one per cent.

$$\epsilon_\theta < 1\% \tag{11}$$

5) The effective clad stresses are less than that which would cause yield of the clad. While the clad has some capability for accomodating plastic strain, the yield strength of irradiation-hardened Zircaloy-4 has been accepted as a conservative design basis,

$$\sigma_{eff.} < \sigma_Y. \tag{12}$$

6) The cumulative strain fatigue cycles are less than the design strain fatigue life. This criterion is known to be consistent

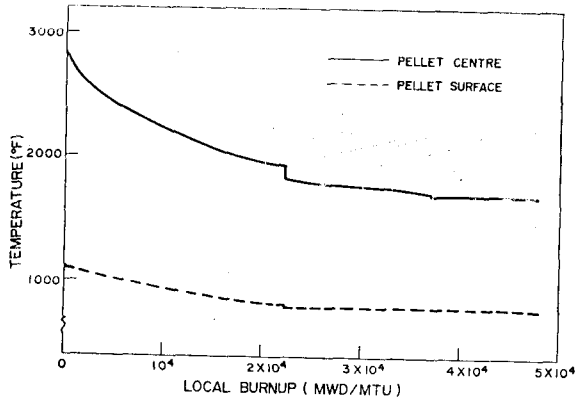

Fig. 4. Temperature Profile in the Pellet at the Slice of Peak Power.

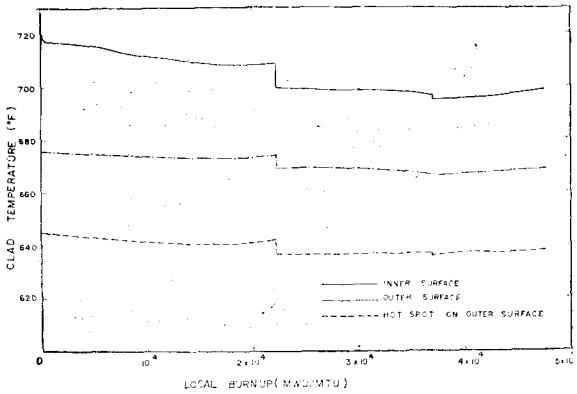

Fig. 5. Temperature Profile in the Clad at the Slice of Peak Power and Clad Hot Spot.

with the proven practice.

Excluding the criterion 6), the FROD 1.0 code provides us with required information for the verification of the design in connection with the prescribed design criteria 1) through 5).

3.3. Results during steady state operation

The profile of maximum temperature in the slice at peak power is calculated and shown in Fig. 4 with respect to its burnup.

Both the centerline and surface temperature of pellet decrease as burnup increases. The decrease in the surface temperature is indebted to the clad creep-down which reduces the gap resitance. Suddun drops shown in the histories are mere consequences of changes in power levels with reloadings. The decrease in centerline temperature is greater than that in the surface temperature of pellet because the thermal conductivity of uranium dioxide is a monotonously decreasing function of temperature within the range of interest in PWR fuels. The benefit is large enough to mask the deterioration of thermal conductivity due to either swelling or cracking of pellet during irradiation. The average rate of decrease in pellet centerline temperature is about 400°F per 10,000 MWD/MTU of peak burnup. It is much greater than that of the melting point of irradiated uranium dioxide [17]. Hence the centerline temperature of pellet is the highest at the beginning of life for steady state operation. Its value is found to be about 3200°F despite that the most pessimistic penalty within two standard deviation levels in modelling uncertainty is included. Thus the fuel melting accident is expected not to occur during the steady state operation. The design criterion 1) is satisfied.

Clad surface temperature does not show any outstanding changes during steady state operation since the reduction in the heat transfer area of clad is only a small amount. The hot spot of clad surface locates at a position of about 0.7 for relative axial height that is higher than the hot spot of pellet centerline by about five feet. The hot spot temperature for limiting the clad external corrosion is not exceeded and the design criterion 2) is satisfied as shown in Fig. 5.

Internal pressure of fuel rod builds up steadily with burnup except at the begin-

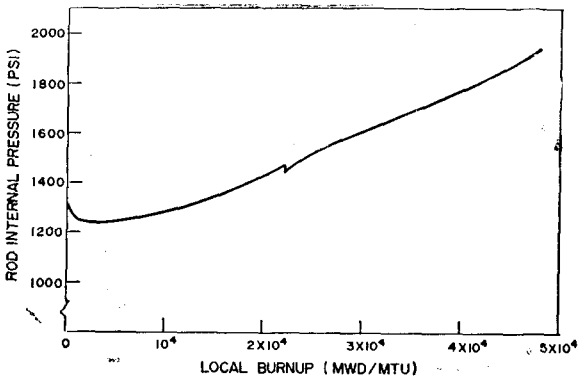

Fig. 6. Buildup of Internal Pressure of Fuel Rod at the Maximum Power

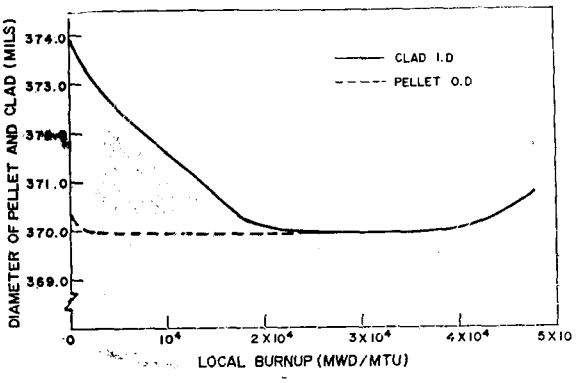

Fig. 7. Deformation History of Pellet and Clad

ning of life and reaches a maximum value at the end of life, as shown in Fig. 6. The internal pressure is reduced to a minimum value at a low burnup due to a decreace in fuel surface temperature and an increase in rod internal void volume owing to fuel densification. The subsequent increase of internal pressure is due not only to fission gas release but also to reduction of gap volume as a result of clad creep-down and fuel swelling. The maximum value at the end of life does not exceed the system pressure of 2250 psia and the design criterion 3) is satistied.

It is elucidated in Fig. 7 that major contribution to the deformation of fuel rod is due to clad creep. The swelling of pellet is not distinguished since the thermal expansion component is dominant along the power history. At the rod-average burnup of about 21,000 MWD/MTU the pellet and the clad start to contact. The history of clad circumferential strain is shown in Fig. 8. The maximum circumferential strain of clad has exceeded 1% during the steady state operation without provoking any safety related problem. The design criterion 4) seems applicable only to transient events where the strain rate is appreciable. Hence the criterion is bypassed for steady-state operation.

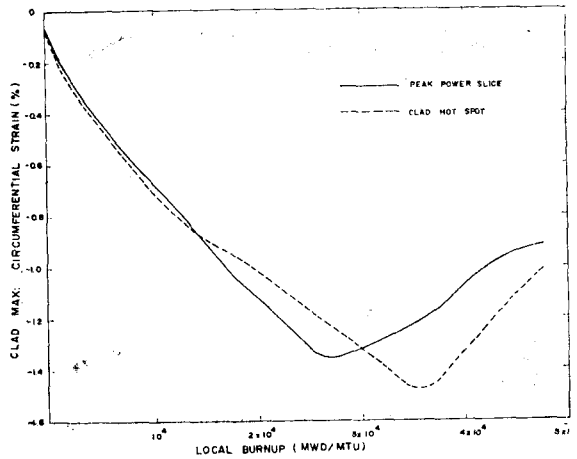

Fig. 8. Circumferential Strain of Clad

Both the radial and hoop components of clad stress are compressive during the first cycle and their magnitude decrease slowly by balancing of boundary pressures and by stress relaxation. After the pellet-clad contact begins, rapid increase in the stress is marked as shown in Fig. 9. Now the significance of pellet-clad mechanical interaction may be glanced at the end of cycle 2 where clad stress varies sensitively with a small change in power level. But further deformation during steady state operation is slow enough to be accomodated by clad creep accompanied with appropriate

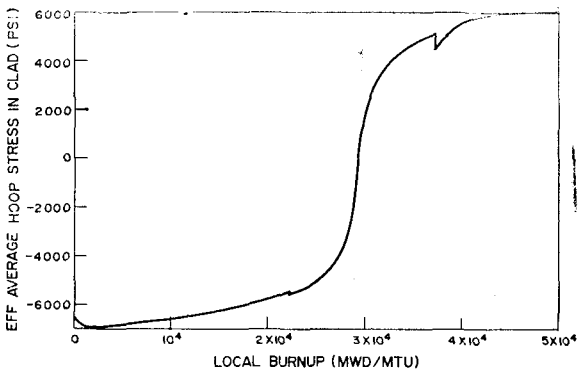

Fig. 9. Buildup of Average Effective Stress in Clad at Peak Power Slice

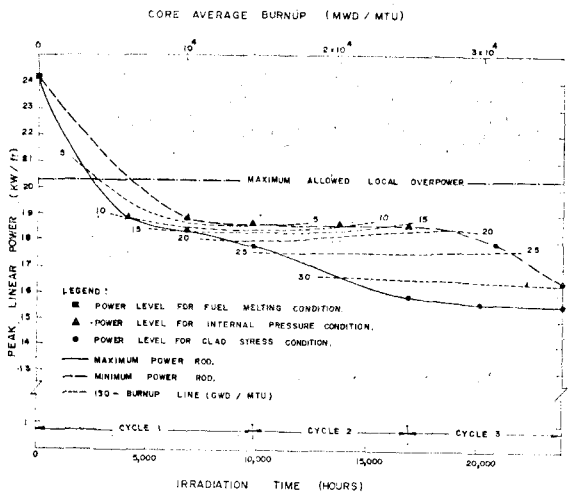

Fig. 10. The Calculated Design Limit of Fuel Rods during the Overpower Condition.

amount of stress relaxation. And the average effective stress of Von Mises criterion does not exceed the yield strength of irradiation-hardened Zircaloy-4. Hence the design criterion 5) is met.

Thus all the prescribed design criteria seem to be met for the fuel rods during the steadystate operation.

3.4. Results during Overpower Transients

The results of overpower case are summarized in Fig. 10. Being based on nominal condition and best statistics, the design limit curves for two power ratings are obtained by plotting the threshold local power level at which the crucial one among the five design criteria is violated during the overpower escalation. The results elucidate that design margins become smaller due to the overpower requirements and decrease with increasing service time.

At early in the beginning of life, the threshold power level is that for fuel melting condition. It is found to be about 24.2 kW/ft for all the fuel rods and is well above the maximum allowed power level of 20.3 kW/ft on which the overpower trip setpoint is based. Therefore the fuel rods are expected to meet all the design criteria under the Condition II events at early in life.

The threshold power levels decrease rapidly during the first several months and thenceforth the rod internal pressure condition, as the crucial criterion, starts to be violated in the allowed power range. As shown in Fig. 10, the threshold power levels for this condition appears to be approximately constant regardless of either the service time or the respective power ratings of followed steady state operation. Even though the internal pressure design criterion is not satisfied, the fuel integrity may be assured because the incremental creep-out of clad during such a short overpower transient will be negligible.

The clad stress condition becomes the crucial criterion at high burnup where pellet and clad are usually in contact or very close as mentioned earlier. The transition time for the clad yielding events is expected to vary from the end of cycle 1 to the beginning of cycle 3 with the respective power ratings. Theceforth the rapid decrease in the threshold power level is noted

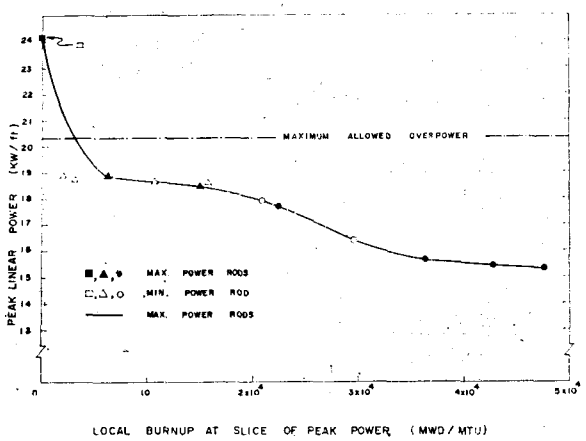

Fig. 11. The Calculated Design Limit during Overpower Condition as a Function of Local Peak Burnup

again for all the fuel rods with further service. For the maximum power rods it is interesting that the threshold power level tends to be stabilzed to a definite value during the cycle 3. It reflects that approximately constant amount of power increase (i.e., the constant amount of the thermal expansion of pellet) will be required to cause clad yielding after the clad creep-down is completed at an equilibrium contact condition between pellet and clad.

As shown, in Fig. 10, by drawing a group of nearly horizontal iso-burnup lines between the two curves, the overpower capability of fuel rods shows a strong dependency on the local burnup rather than on the service time. And the apparent relationship is clarified in Fig. 11 by reproducing Fig. 10 with respect to local burnup.

Thus the calculated design limit under the Condition II events does not agree with the assessments in the Final Safety Analysis Report at the high burnup[16]. The discrepancy may be attributed, in part, to the input uncetainties in either the power histories for later two cycles or the axial power shape under the ANS condition II events. And there are also some uncertainties in modelling due to the localized stress concentration in the clad and the potential iodine stress corrosion cracking penalties[18, 19]. On the other hand, there would be a benefit that maximum local power peakings under the ANS Condition II events (realistic values of which are lacking at the time of this study) may not be so high after having experienced an appropriate burnup. Hence the occurrence of design violation can hardly be determined by the present calculation only.

However the possibility of clad yielding events at high burnup may not be overlooked because all the later cycles will have such a high equilibrium burnup and the clad material would be very brittle at that time.

Therefore it seems valuable to verify the overpower allowance in the equilibrium core in the further study.

4. Conclusion

A computer code for mechanical and thermal analysis of oxide fuel rods has been developed and the code, FROD 1.0 is capable for parametric design study and performance prediction.

An application is made for the performance prediction of fuel rods loaded in the first core of Go-ri Nuclear Power Plant unit 1. For the steady state operation, all the fuel rods are expected to design criteria throughout their lives. For the overpower events which start from steady state operation, it is found that the overpower capability of fuel rods may be deteriorated as a strong function of local burnup And the more detailed verification of the over-

power allowance in the equilibrium core is recommended to include the calculations of1) the accurate steady state power histories for the later two cycles and the axial power shapes during the overpower transients, 2) localized stress concentration in the clad and potential iodine stress corrosion cracking penalties, 3) realistic values of maximum local power peakings under the overpower transients at high burnup.

Acknowledgement

The authors express their deep thanks to Dr. P.E. Juhn, Acting Head of the Reactor Core Design and Systems Engineering Division in Korea Atomic Energy Research Institue, for his invaluable advice and discussion throughout the course of this research work.

Nomenclature

a pellet radius
b clad outer radius
a', b' fictitious values of a and b, respectively.
c clad outer radius
E^{I} Young's modulus of fuel
E^{II} Young's modulus of clad
$E_{cont.}$ strength coefficient
F_Q^T, F_{XY}^N, F_Z^N, F_U^N and F_Q^E are hot channel factors explained in text
$f(r)$ normalized power depression function
k thermal conductivity of pellet
L pellet stack length
$\dot{m}$ mass flow rate of coolant
$P_{cont.}$ contact pressure
P_i internal pressure of fuel rod
P_s primary coolant system pressure
q''' volumetric heat generation
q_s''' volumetric heat generation rate at pellet surface
q_c'' surface heat flux at clad outer surface
r variable of radius
T temperature
T_0 temperature at pellet centerline
T_b temperature at pellet outer surface
T_c temperature at clad outer surface
T_f mixed-mean coolant temperature
z variable of height
ϵ_θ circumferential strain
σ_y yield strength of clad
ν^{I} Poisson's ratio of fuel
ν^{II} Poisson's ratio of clad

REFERENCES

1. H. Stehle and H. Assmann, "The Depencence of Inreactor UO_2 Densification on Temperature and Microstructure," J. of Nucl. Mater., Vol. 52, 1974 pp. 303.
2. J.R. Fagan and J.O. Mingle, "The Effect of Axial Heat Conduction in Fuel Plates on Maximum Heat Flow Rates and Temperatures," Nucl. Sci. Eng., Vol. 18, 1964, pp. 443.
3. C.S. Rim, "Neutronic and Thermal Analysis of Nuclear Fuel," Sc. D. Thesis, MIT, 1969.
4. J. Wordsworth, "IAMBUS-1-A Digital Compu ter Code for the Design, In-pile Performance Prediction and Post-irradiation Analysis of Arbitrary Fuel Rods", Nucl. Eng. Des., Vol. 31, 1974, pp. 325.
5. A.M. Ross and R.S. Stoute, "Heat Transfer Coefficient Between UO_2 and Zirealoy-2," AECL-1552, June, 1962.
6. J.M. Kendall, M.B. Hsu, C. Chan and T.J. Dwyer, "Blowdown Effects on a Fuel Rod", in "Fuel Element Analysis", A.S.M.E. Special Publication, 1975, pp. 39.
7. L. Lunde, "Special Features of External Corrosion of Fuel Cladding in Boiling Water Reactors, Nucl. Eng. Des., Vol. 52, 1975, pp. 187.
8. F.W. Dittus and L.M.K. Boelter, Univ. Calf. Publs. Eng., Vol. 2, 1930, pp. 443.
9. J. Weisman, "Heat Transfer to Water Flowing Parallel to Tube Bundles", ucl. Sci. Eng.,

Vol. 6, 1959, pp. 78.

10. J. A. L. Robertson, "Irradiation Effects in Nuclear Fuels", ANS-USAEC Monography, Gordon and Breach, Inc., 1969, pp. 151.
11. F. Anselin and W. E. Baily, "The Role of Fission Products in the Swelling of Irradiated UO_2 and (U, Pu) O_2 Fuels", Trans. Am. Nucl. Soc., Vol. 11, 1968, pp. 515.
12. Che-yu Li, S. R. Pati, R. B. Poepple, R. O. Scattergood and R. W. Weeks, Nucl. Appl. Tech., Vol. 9, 1970, pp. 188.
13. P. E. Macdonald and J. Weisman, "Effect of Pellet Cracking on Light Water Reactor Fuel Temperatures", Nucl. Tech., Vol. 31, 1976, pp. 357.
14. C. F. Bonila, "Nuclear Engineering", McGraw-Hill Book Co., N. Y., 1957, pp. 574.
15. Z. Zudans, T. C. Yen and W. H. Steigelmann, "Thermal Stress Techniques in the Nuclear Industry", American Elsevier Publishing Co., 1965, pp. 235.
16. Korea Electric Company, "The Final Saftety Analysis Report, Go-ri Nuclear Power Plant, Unit No. 1", 1976.
17. J. A. Christensen, R. J. Allio and A. Biancheria, "Melting Point of Irradiated Uranium Dioxide", WCAP-6065, WAPD, 1965, pp. 8.
18. W. J. Penn, R. D. Lo and J. C. Wood, "CANDU Fuel-Power Ramp Performance Criteria", Nucl. Tech. Vol. 35, July. 1977, pp. 249.
19. J. T. A. Roberts, E. Smith, F. Fuhrmam and Cubicciotti, "On the Pellect-Cladding Interaction Phenomenon", Nucl. Tech. Vol. 35, Mid-Aug. 1977, pp. 131.